

PAPER • OPEN ACCESS

Microstructure and Structure of $\text{LaMnO}_3/\text{Mn}_2\text{O}_3$ Film Prepared by Electrodeposition Method

To cite this article: Gede Yudharma *et al* 2019 *IOP Conf. Ser.: Mater. Sci. Eng.* **546** 042052

View the [article online](#) for updates and enhancements.

Microstructure and Structure of $\text{LaMnO}_3/\text{Mn}_2\text{O}_3$ Film Prepared by Electrodeposition Method

Gede Yudharma¹, I N Rahman¹, Budhy Kurniawan^{1*}, Bambang Soegijono¹ and Setia Budi²

¹Department of Physics, Faculty of Mathematics and Natural Sciences, Universitas Indonesia, Indonesia

²Department of Chemistry, Faculty of Mathematics and Natural Sciences, Universitas Negeri Jakarta, Indonesia

*Corresponding author : budhy.kurniawan@sci.ui.ac.id

Abstract. In this study, $\text{LaMnO}_3/\text{Mn}_2\text{O}_3$ (LMO/MO) film are synthesized using electrodeposition method on SS 316L substrate. The preparation LMO/MO for this electrodeposition was carried out with a concentration of La^{3+} and Mn^{2+} between 50 - 150 mM solution. Electrodeposition results show that with a currents variation of 0.1; 0.5; 1; 2.5 mA, LaMnOH_x and MnOH_x compounds have been formed. It is also observed that an increasing current are followed by increasing in the composition of the La atom. The good thickness of sample occurs at currents of 1 mA. The sample was then heated at 800°C for 4 hours. The X-ray diffraction (XRD) analysis shows that the sample forms LaMnO_3 and Mn_2O_3 phase with ratio composition of 1.79% and 98.21%.

1. Introduction

Lanthanum manganite research has been a concern, especially in the application in solid oxide fuel cell [1] and giant magneto resistance materials [2]. Various methods have been developed to synthesize LaMnO_3 , such as the conventional solid-state reaction [3], coprecipitation [4], sol-gel [5], spin coating [6], sputtering [7], Pulsed Laser Deposition [8], chemical vapour deposition (CVD) [9], and electrodeposition [10]. Nanomaterials based on LaMnO_3 can provide novel properties like enhanced magnetization, quantum effects or improved mechanical properties. By properly tuning the particle size, it is possible to optimize the desired properties of these materials [11]. Electrodeposition offers a potentially powerful technique for preparing thin oxide films with controlled thicknesses and surface morphologies. The key advantages of this deposition technique include a wide range of oxide films can be prepared without a vacuum, using simple and low-cost equipment [12].

In earlier research, Matsumoto *et al* [13] have shown in their studies that even though Ln^{3+} ions do not participate in any oxidation reactions, they can be incorporated into the anodically grown oxide-hydroxide films of Mn and Co provided a very high Ln^{3+}/M ratio (10^2 – 10^3) which is maintained in the bath. Therese *et al* [14] employed the electrogeneration of base by the cathodic reduction of a mixed-metal ($\text{Ln}^{3+} + \text{M}^{2+}/\text{M}^{3+}$) nitrate bath in a divided cell. Bidrawn *et al* [15] have done electrodeposited Sr-doped LaMnO_3 into a porous substrate of Y_2O_3 -stabilized ZrO_2 and determined electrochemical performance of a composite cathode for SOFCs. More recently, Park *et al* conduct research on a bilayered $\text{LaMnO}_3/\text{Co}_3\text{O}_4$ coating for SOFC applications which is fabricated by a three-step process: (i)



electrodeposition of metallic Co; (ii) chemically assisted electrodeposition of LaMnOH_x in a divided cell electrodes; and (iii) thermal conversion of $\text{LaMnOH}_x/\text{Co}$ to $\text{LaMnO}_3/\text{Co}_3\text{O}_4$. [10]

In this study, we prepared a thin film of $\text{LaMnO}_3/\text{Mn}_2\text{O}_3$ on electrodeposition to a stainless-steel substrate. Moreover, the sintering temperature should be limited to a level lower than 1000°C to prevent severe oxidation and possible phase transformation of stainless steels [12]. The LaMnO_3 film was grown on the substrate at room temperature by controlling the current deposition using a galvanostat deposition approach. As far as we know, there is no research on the electrodeposition of LaMnO_3 thin films and their magnetic properties.

2. Experimental

Stainless steel substrate (SS 316L), which was used as a work electrode, was cut off with a dimension of $10\text{ mm} \times 30\text{ mm}$. The substrate was polished with 400-, 800-, and 1200-grid SiC papers and then cleaned with an ultrasonic device for 10 minutes, rinsed with 96% alcohol to remove dirt and dust. All electrodeposition processes were performed in a three-electrode cell using a platinum wire as a counter electrode and Ag/AgCl as a reference electrode. Cathodic current density and deposition time are 0.1; 0.5; 1; 2.5 and 5 mA/cm^2 for 3–20 min. The applied currents were controlled with an eDAQ potentiostat model EA163 with galvanostat and recorder 401 model. Stoichiometric amount of $\text{La}(\text{NO}_3)_3 \cdot 6\text{H}_2\text{O}$ (Merck, 99.99%), $\text{Mn}(\text{NO}_3)_2 \cdot 4\text{H}_2\text{O}$ (Merck, 98.5%) in deionized water was prepared. To find the optimum conditions for the fabrication of perovskite oxide, electrodeposition was conducted in solutions with various precursor concentrations. The concentrations of La^{2+} and Mn^{3+} were varied between 20 mM and 150 mM. The solution pH was adjusted to 4 by the addition of 0.1M HCl. The oxide films prepared on the electrode were washed with distilled water, followed by drying at room temperature and finally, heat-treated in air at 800°C with a temperature increase time of 2 hours and a holding time of 2 hour. The morphology of the samples was measured using X-pert panalytical instrument. The surface chemistry was examined by energy dispersive X-ray spectroscopy (EDS Oxford Instrument).

3. Results and Discussion

Electro-reduction of an aqueous nitrate solution have been described by Therese [14] and Sasaki *et al* [13]. The reactions can be divide in two, one reaction is related to nitrate reduction and the other related to hydrogen evolution:



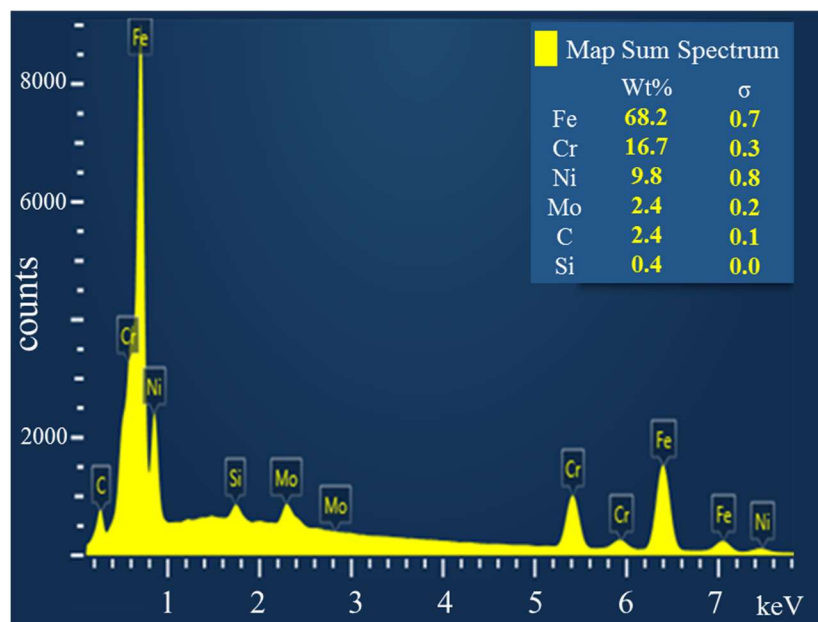
Both reactions release OH^- ions and lead to an increase in pH close to the electrode. Consequently, metal ions get electrodeposited on the cathode as hydroxide/oxide coatings in which the deposit thickness can be varied from nanometers to micrometers.



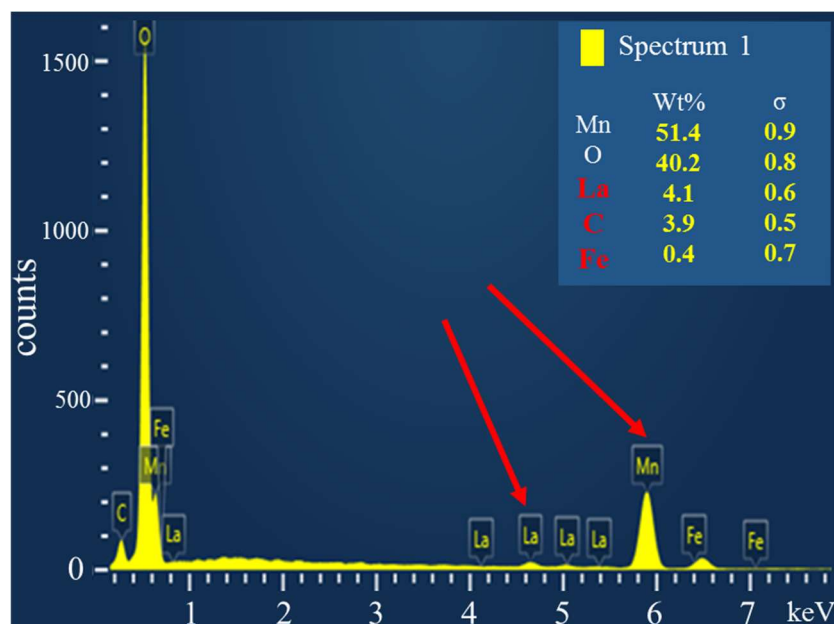
The nitrate reduction reaction should occur at negative potential ($-0.13\text{ V vs Ag/AgCl}$) as compared with that of mangan(II) electrodeposition ($-1.39\text{ V vs Ag/AgCl}$). When electrodeposition is performed in the potential range between -1.0 and -0.7 V vs Ag/AgCl , the over voltage for nitrate reduction should be much larger than those for mangan deposition; thus, nitrate reduction would be dominant, leading to the formation of metal hydroxide precipitates. The measured potentials are much higher than the reduction potentials of La^{3+} ($-2.58\text{ V vs Ag/AgCl}$) and Mn^{2+} ($-1.39\text{ V vs Ag/AgCl}$), which indicates that La^{3+} and Mn^{2+} would not be electrochemically reduced to their metal phase [10].

The EDS test results show that the deposition process for La and Mn can be done simultaneously, as seen from the La and Mn spectra in Figure 1 and Figure 2. In Figure 1a, it can be seen that the EDS

results for the substrate have no La and Mn elements, whereas Figure 1b (substrate results after electrodeposition), La and Mn were formed in the substrate. This indicates that the results of electrodeposition with various concentration or ratio of La^{3+} / Mn^{2+} succeeded in positioning La and Mn. The amount of La is still much smaller compared to the deposited Mn ion. The result from synthesized sample using current variation of 0.1; 0.5; 1.0; 2.5 and 5.0 with a deposition time of 10 minutes and a concentration of solution namely $[\text{La}^{3+}] = 50 \text{ mM}$ and $[\text{Mn}^{2+}] = 150 \text{ mM}$ is presented in the Figure 3. The four samples were characterized by EDS while the fifth sample with a 5-mA current was not characterized because the deposit did not stick to the substrates. Processing parameters used for cathodic current density can be conducted at a relatively high current density [10].



(a)



(b)

Figure 1. EDS for (a) Substrate (b) Substrate after electrodeposition

On the other hand, the chemically assisted electrodeposition of LaMnOH_x requires a relatively low current density to produce a dense, crack-free, and adhesive layer. At high cathodic currents, the rate of NO_3^- reduction (OH^- generation) would become much faster than that of LaMnOH_x precipitation, which causes the excessive growth of the high pH region and results in the formation of deposits with low density and poor adhesion strength [12]. Figure 3a shows working electrode surface being covered with the oxide film. With current density of 0.1 mA indicating that the conductivity of the deposited oxide film was low.

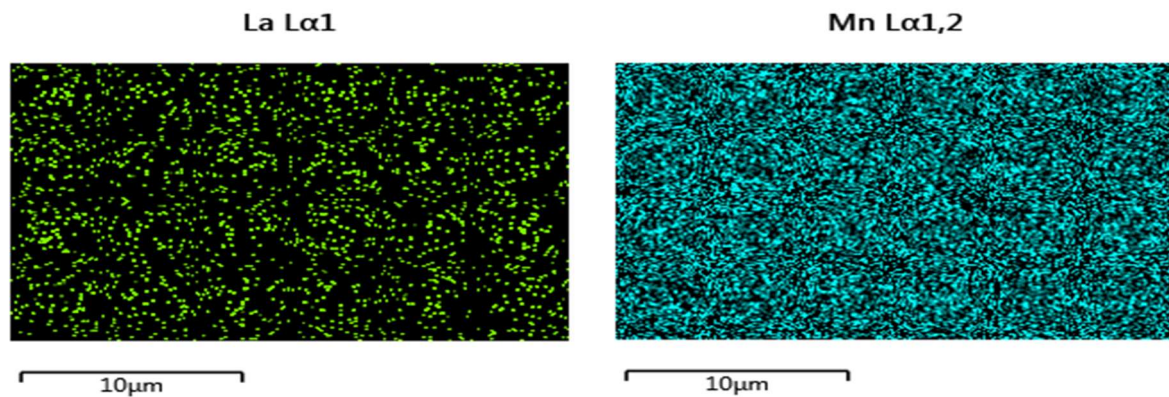


Figure 2. Mapping elements: La and Mn

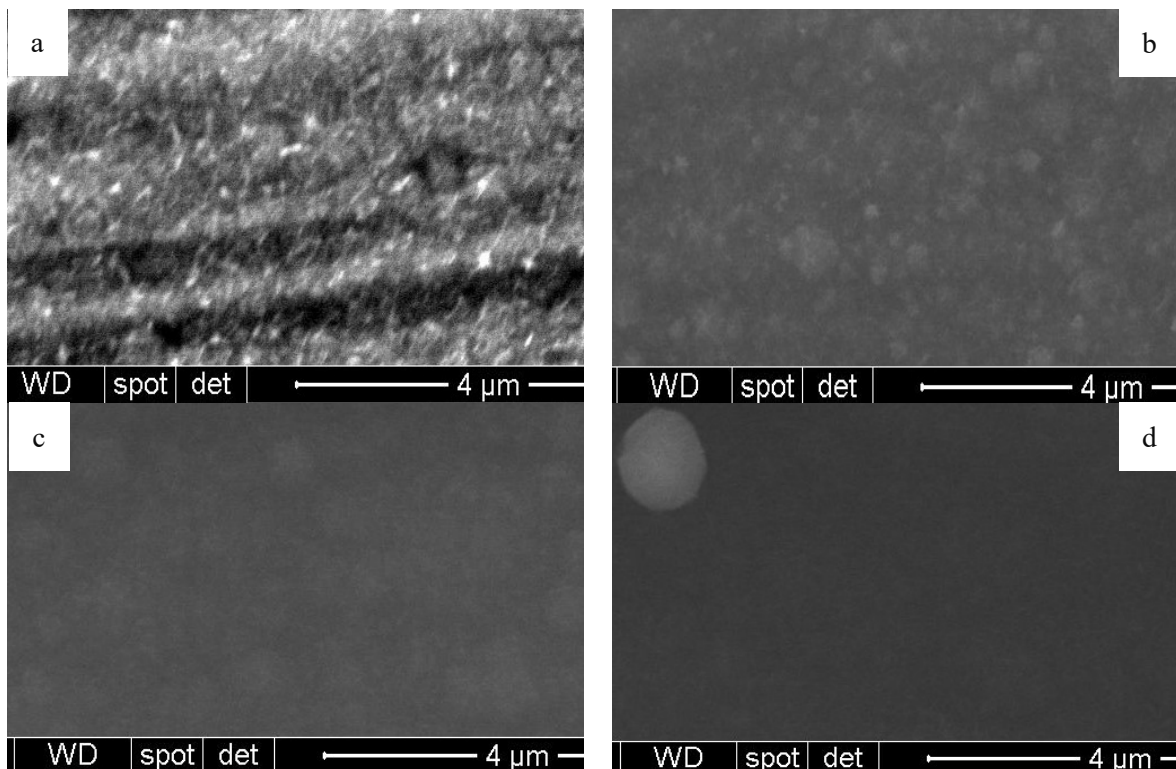


Figure 3. The electrodeposition result for 10 minutes with $[\text{La}^{3+}] = 50 \text{ mM}$ and $[\text{Mn}^{2+}] = 150 \text{ mM}$ and current variation of a). 0.1 mA, b). 0.5 mA, c). 1 mA, d). 2.5 mA.

According to Matsumoto *et al* [16], the oxide film under the galvanostatic electrolysis observed as a function of the decrease of the current density. When the current density was low, the conductivity is also low. The electrodeposition results show that current variations of 0.1, 0.5, 1 and 2.5 mA gives LaMnOH_x and MnOH_x compounds. Moreover, an increase current is followed by increase in the

composition of the La atom. The good thickness of sample occurs at currents of 1 mA. Figure 4 shows the atomic percentage of La in the oxide film which was analyzed by EDS as a function of the $[\text{La}^{3+}]/[\text{Mn}^{2+}]$ ratio in the solution. The La is relatively more difficult to grow in the substrate than the Mn. The atomic percentage of La in the oxide increases with an increase in the $[\text{La}^{3+}]/[\text{Mn}^{2+}]$ ratio in the solution. For the solution with $[\text{La}^{2+}] = 20$ mM and $[\text{Mn}^{2+}] = 140$ mM, the amount of La formed on the substrate was 0.19%. When the concentration ratio is increased, the number of formed La is also increase. For $[\text{La}^{3+}] = 100$ mM and $[\text{Mn}^{2+}] = 150$ mM, the amount of La formed was 0.77%, while for $[\text{La}^{3+}] = 200$ mM and $[\text{Mn}^{2+}] = 150$ mM, the amount of formed La was 0.88%. This is consistent with author's previous research, despite the use anodic electrosynthesis during synthesizing process[17]. The atomic ratio of La/Mn in the oxide film which was analysed using ICP spectroscopy as a function of the $[\text{La}^{3+}]/[\text{Mn}^{2+}]$ ratio in the solution. The atomic ratio of La/Mn in the oxide increases with an increase in the $[\text{La}^{3+}]/[\text{Mn}^{2+}]$ ratio in the solution. Samples with $[\text{La}^{2+}] = 50$ mM and $[\text{Mn}^{2+}] = 150$ mM and current variation of 1 mA appear to form a fairly good layer compared to the others. For this reason, the sample was then characterized by XRD to determine the structure and phase formed.

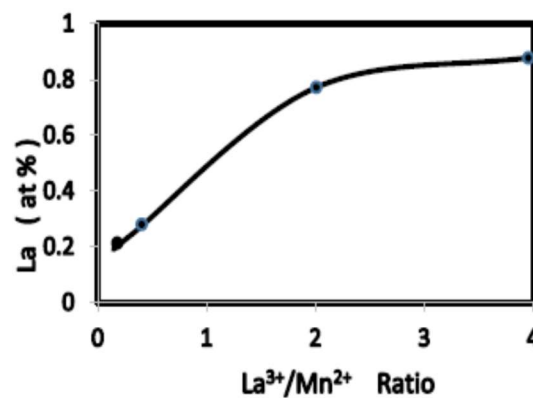


Figure 4. Atomic percentage of La as a function of $[\text{La}^{3+}]/[\text{Mn}^{2+}]$ ratio

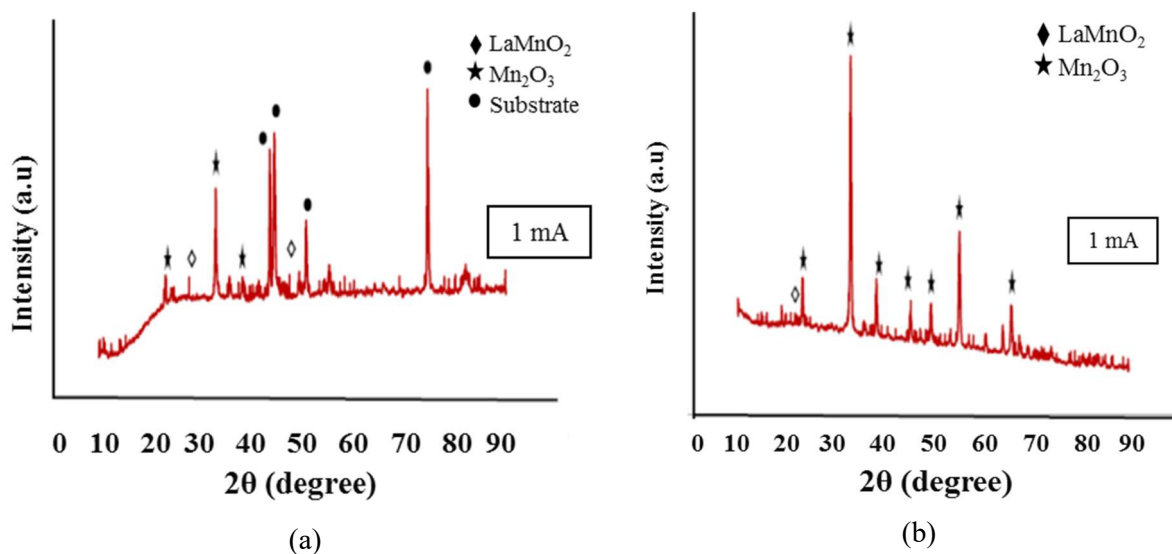


Figure 5. Refined XRD pattern for (a) electrodeposition results on SS 316L substrate and (b) electrodeposition results after being scraped off SS 316L substrate

The refined XRD pattern is presented in Figure 5. The result of deposition composed of LaMnO_3 and secondary phases of Mn_2O_3 (denoted by symbols “ \diamond ” and “*”, respectively). Park *et al* [10] has carried out research with a composition La^{2+} and Mn^{2+} between 20 -180 mM. Park found that single phase LaMnO_3 occurs when the composition of $[\text{La}^{2+}] = 20$ mM and $[\text{Mn}^{2+}] = 140$ mM. Moreover, other phases are also formed, such as La_2O_3 , La_2CrO_6 , Mn_3O_4 , and Crofer. While according to Sasaki study, when LMO samples was heated at 700°C and 800°C , it formed Mn_2O_3 phase and LaMnO_3 phase, respectively, with a denominational current of 0.5 mA [13]. The XRD analysis shows that the sample was transformed into LaMnO_3 and Mn_2O_3 phases with composition ratio of 1.79% and 98.21%.

4. Conclusion

The synthesis of Lanthanum manganite using electrodeposition process have been studied. Electrodeposition of Lanthanum manganite has been carried out by varying the concentration of the solution. By increasing the ratio of $[\text{La}^{3+}]/[\text{Mn}^{2+}]$, La atoms were increasingly deposited. Rietveld refinement result shows that all samples were composed of LaMnO_3 and secondary phases of Mn_2O_3 .

Acknowledgments

This work was supported by Universitas Indonesia under research grant PIT 9 with contract number NKB-0021/UN2.R3.1/HKP.0500/2019, with the title of “Sintesis dan Karakterisasi Material Fungsional Berbasis Perovskite Manganite dan MoS_2 Sebagai Material Maju”.

(Rev. Fac. Ing.) Vol. 26 (44), pp. 123-

References

- [1] J. Fleig, K. D. Kreuer, J. Maier. 2003. “Ceramic Fuel Cells,” in Handbook of Advanced Ceramics: Materials, Applications, Processing and Properties.
- [2] K. Steenbeck, T. Eick, K. Kirsch, H. G. Schmidt, E. Steinbeiß. 1998. Appl. Phys. Lett. 71 968.
- [3] M. Roy and S. Sahu. 2013. *J. Electroceramics* **31** (3-4) 291.
- [4] I. Maurin, P. Barboux, Y. Lassailly, J. P. Boilot. 1998. *Chem. Mater.* **10** (6) 1727.
- [5] Z.B.H. Aga and S.R. Ramanan. 2012. *J. Electroceramics* **28** (2-3) 109.
- [6] J.A. Mera-Córdoba, M.A. Mera-Córdoba, C.A. Córdoba-Barahona. 2017. *Rev. Fac. Ing.* **26** (44) 123.
- [7] V. Franco, J.S. Blázquez, B. Ingale, A. Conde. 2012. *Annu. Rev. Mater. Res.* **42** 305.
- [8] J.N. Davis, K.F. Ludwig, K.E. Smith, J.C. Woicik, S. Gopalan, U.B. Pal, S.N. Basu. 2017. *J. Electrochem. Soc.* **164** (10) F3091.
- [9] T. Nakamura, T. Nishimura, R. Tai, K. Tachibana. 2005. *Mater. Sci. Eng. B: Sol. State Mater. Adv. Technol.* **118** (1-3) 253.
- [10] B.K. Park, R.H. Song, S.B. Lee, T.H. Lim, S.J. Park, W.C. Jung, J.W. Lee. 2017. *J. Pow. Sour.* **348** 40.
- [11] N. Das, D. Bhattacharya, A. Sen, H.S. Maiti. 2009. *Ceram. Int.* **35** (1) 21.
- [12] B K. Park, R H. Song, S B. Lee, T H. Lim, S J. Park, C.O Park, J W. Lee. 2015. *J. Electrochem. Soc.* **162** (14) F1549.
- [13] T. Sasaki, Y. Matsumoto, J. Hombo, Y. Ogawa. 1991. *J. Sol. State Chem.* **91** 61.
- [14] G.H.A. Therese and P.V. Kamath. 1998. *Chem. Mater.* **10** (11) 3364.
- [15] F. Bidrawn, J.M. Vohs, R.J. Gorte. 2010. *J. Electrochem. Soc.* **157** (11) B1629.
- [16] Y. Matsumoto, T. Morikawa, H. Adachi, J. Hombo. 1992. *Mater. Res. Bull.* **27** (11) 1319.
- [17] Y. Matsumoto, T. Sasaki, J. Hombo. 1991. *J. Electrochem. Soc.* **138** (5) 1259.